Temperature-, molar ratio- and counterion-effects on the crystal growth of bipyridinium-bis(alkylcarboxylic acid)–crown ether pseudorotaxanes†

Gellert Mezei, Jeff W. Kampf and Vincent L. Pecoraro*

Received (in St Louis, MO, USA) 20th October 2006, Accepted 4th January 2007
First published as an Advance Article on the web 8th February 2007
DOI: 10.1039/b615273b

Five new dicarboxylic acid-functionalized pseudorotaxanes, comprised of a bis(1,5-naphtho)-38-crown-10 ring-component and a *N*,*N*′-di(*n*-carboxyalkyl)-4,4′-bipyridinium dihexafluorophosphate (n = 4 or 5, alkyl = butyl or pentyl) rod-component, have been synthesized and characterized by UV-Vis and ^{1}H-NMR spectroscopic, ESI-MS and/or X-ray crystallographic methods. Depending on the temperature of crystallization and the molar ratio between the *N*,*N*′-di(4-carboxybutyl)-4,4′-bipyridinium rod and the crown ether, three different polymorphs were obtained. In the case of the *N*,*N*′-di(5-carboxypentyl)-4,4′-bipyridinium rod, two different pseudorotaxane-structures were obtained at different temperatures and in the presence of one or two different counterions. The latter one is an unprecedented example of a pseudorotaxane in which the bipyridinium rod is not sandwiched in-between the crown ether ring's two naphthalene units, as expected, but forms intermolecular π–π interactions with neighboring pseudorotaxanes.

Introduction

Presently, considerable attention is focused on the preparation of bifunctional molecules or materials. As part of our ongoing research on functional metallacrown complexes, we are exploring the chemistry, properties and possible applications of supramolecular assemblies formed between metallacrowns and rotaxanes/pseudorotaxanes. Metallacrowns are cyclic inorganic complexes analogous to crown ethers, often having an M–N–O instead of a C–C–O repeat unit which leads to a structure with a high metal density. The single molecule magnet behavior displayed by several metallacrowns is an interesting consequence of the close proximity of numerous metals with high magnetoanisotropy.[1] These large metallamacrocycles have sizes and shapes reminiscent of porphyrins and texaphyrins. Rotaxanes and pseudorotaxanes, supramolecules in which a ring-like component can slide along a threaded rod-like component, have received increased attention in recent years due to their potential of being developed into molecular devices and machines.[2] Examples of such rotaxane-based devices include molecular shuttles,[3] muscles,[4] elevators,[5] nanovalves,[6] information storage devices[7] and components for molecular electronics such as molecular switches[8] and single-molecule transistors.[9] The next stage in the engineering of more complex molecular machinery would be the assembly of two or more such devices into discrete supramolecular entities. The construction of a device incorporating a single molecule magnet and a rotaxane is particularly appealing.

Departments of Chemistry and Biophysics, The University of Michigan, Ann Arbor, Michigan, USA. E-mail: vlpec@umich.edu; Fax: +1 734 936 7628; Tel: +1 734 763 1519

† Electronic supplementary information (ESI) available: Variable-temperature ^{1}H-NMR spectra (Fig. S1) and ESI-MS spectrum (Fig. S2) for **4**·2PF_6–BN-38-C-10. See DOI: 10.1039/b615273b

The synthesis of pseudorotaxanes is not a trivial task, for the spontaneous, statistical threading of macrocycles onto rod-like molecules is a highly inefficient strategy that has never been reported to yield a stable, isolable pseudorotaxane. Therefore, a specific template is needed in order to hold the ring- and rod-molecules together, and often two bulky, terminal stoppers (such as porphyrins) are also required to prevent the macrocycle from slipping off the rod-molecule. Non-covalent interactions such as hydrogen bonding,[10] aromatic interactions[11] (both with and without additional electrostatic interactions) and coordination bonds[12] have all been successfully used as templates for the preparation of stable pseudorotaxanes. For our purposes, we have chosen the bipyridinium dication–dinaphthalene crown ether synthon, which is known to form stable and readily identifiable pseudorotaxanes[13] and catenanes.[14] In this case the driving force for the assembly of the pseudorotaxane is the combined effect of π–π stacking and electrostatic interactions between the electron-deficient bipyridinium dication and the electron-rich crown-ether. The resulting charge transfer imparts a deep-red color to the pseudorotaxane and serves as a visual indicator for the self-assembly process.

In order to assemble the two components in a pre-determined fashion, both the metallacrown and pseudorotaxane need to have specific anchor-points. A convenient anchor-point on metallacrowns is the highly-charged, hard Ln(III) ion sequestered in the center of 15-MC-5 complexes, which is known to preferentially bind carboxylates. A linear molecule with carboxylate groups at the two ends was, therefore, envisioned as a potential rod-component for the construction of a pseudorotaxane that can be intercalated between two metallacrown single-molecule magnets. During the course of these studies evaluating the pseudorotaxane portion of the construct, we observed that crystals of different morphology could be isolated, which revealed differential threading of the rings as a function of crystallization conditions.

Polymorphism—the phenomenon wherein the same substance exhibits different crystal packing arrangements[15]—has been recognized to be of major importance to the economic viability of many industrial processes, with strong impact on the pharmaceutical, paints and pigments, explosives, electronics and food industries.[16] Therefore, understanding and controlling the formation of polymorphs is crucial for the preparation of materials having the desired physico-chemical properties. Towards this aim, extensive research has been devoted to the study of polymorphs.[17] Herein, we describe the synthesis, characterization and polymorphism of five new pseudorotaxanes containing dicarboxylate rod-components.

Results and discussion

Synthesis of the bipyridinium-bis(alkylcarboxylic acid) rod molecules

The bipyridinium-based rod molecules were prepared starting from 4,4′-bipyridine (Scheme 1). In the first step, 4,4′-bipyridine was reacted with ethyl 4-bromobutyrate or ethyl 5-bromovalerate, respectively, resulting in the attachment of the alkyl-carboxylate ethyl ester arms. As the bipyridinium cation is formed, the product precipitates out as an insoluble yellow powder and can easily be separated from the mother liquor by filtration. However, ^{1}H-NMR spectroscopy indicated that it contains ~10% impurity (possibly mono-substituted bipyridinium-derivative or its hydrobromide and bipyridinium-bis(hydrobromide), the source of the HBr being the partial dehydrobromination of the bromo-alkyl-ester that can occur under the given reaction conditions). Recrystallization from MeOH-solution by precipitating with Et_2O affords the pure product. The ethyl ester was then hydrolyzed with aqueous HBr. Evaporation of the solution is necessary for complete hydrolysis, as shown by ^{1}H-NMR spectroscopy. The dicarboxylic acid was redissolved in water and treated with a concentrated aqueous NH_4PF_6 solution, resulting in counter-anion exchange and precipitation of the hexafluorophosphate salt, which, in turn, dissolves readily in organic solvents such as CH_3CN and acetone.

Synthesis and crystal growth of the pseudorotaxanes

Since the bis(1,5-naphtho)-38-crown-10 (BN-38-C-10) is only soluble in halogenated solvents such as $CHCl_3$ or CH_2Cl_2 (which do not dissolve the bipyridinium-dication), a mixture of solvents was used for the preparation of the pseudorotaxanes. Thus, a BN-38-C-10 solution in $CHCl_3$ was added to a solution of *N*,*N*′-di(4-carboxybutyl)-4,4′-bipyridinium dihexafluorophosphate (**2**·2PF_6) in CH_3CN, resulting in the formation of a deep-red solution. It was found that a 2 : 1 CH_3CN–$CHCl_3$ mixture was needed in order to get a clear solution; with other ratios precipitation of either one or the other component is observed. For the same reason, crystals of the pseudorotaxane cannot be grown by solvent evaporation, as the two solvents have different vapor pressures and $CHCl_3$ (vp = 160 mm Hg per 20 °C) evaporates faster than CH_3CN (vp = 73 mm Hg per 20 °C), producing crystals of the crown ether. When $CHCl_3$ was exchanged for CH_2Br_2 (vp = 35 mm Hg per 20 °C), in which case the acetonitrile evaporates first, crystals of the bipyridinium compound were obtained. Diethyl ether vapor-diffusion into the 2 : 1 CH_3CN–$CHCl_3$ mixture, however, proved to be successful in growing crystals of the pseudorotaxanes (Scheme 2). Using a 1 : 1 ratio of bipyridinium rod–crown ether, red crystals of (**2**)(BN-38-C-10)$(PF_6)_2$ (pseudorotaxane **Ia**) were obtained in ~5% yield by room temperature (20 °C) vapor-diffusion. In an attempt to increase the yield, the experiment was repeated with a 2 : 1 molar ratio of bipyridinium rod–crown ether and the crystal-growing process was carried out at both room temperature and −20 °C. At room temperature, red crystals of (**2**)(BN-38-C-10)$(PF_6)_2$ (pseudorotaxane **Ib**) formed in ~70% yield, while at −20 °C red crystals of (**2**)(BN-38-C-10)$(PF_6)_2 \cdot 4CH_3CN$ (pseudorotaxane **Ic**) were obtained in >90% yield.

Description of the crystal structures

Pseudorotaxanes Ia–c. In the crystal structures of **Ia–c**, the rod-component is threaded through the crown ether ring so that the electron-deficient bipyridinium moiety is sandwiched in-between the two electron-rich naphthalene moieties, giving rise to the pseudorotaxane-type structures (Fig. 1–3). The interplanar separation between the essentially coplanar donor and acceptor units is 3.35 Å for **Ia** and **Ib** and 3.40 Å for **Ic**. The bipyridinium-based rod can assume different orientations relative to the crown-ether ring, and, based on the reaction conditions, three polymorphs have been isolated. As illustrated in Fig. 4, the difference between the structures of **Ia** and **Ib** (both crystals obtained at room temperature) is in the conformation of the crown ether rings and orientation of the alkyl-carboxylate arms relative to the crown ether, while the orientation of the bipyridinium moiety relative to the two naphthalene units of the crown ether is identical. The structure of **Ic** is different from the structures of **Ia** and **Ib** in that the rod-component here assumes an opposite orientation relative

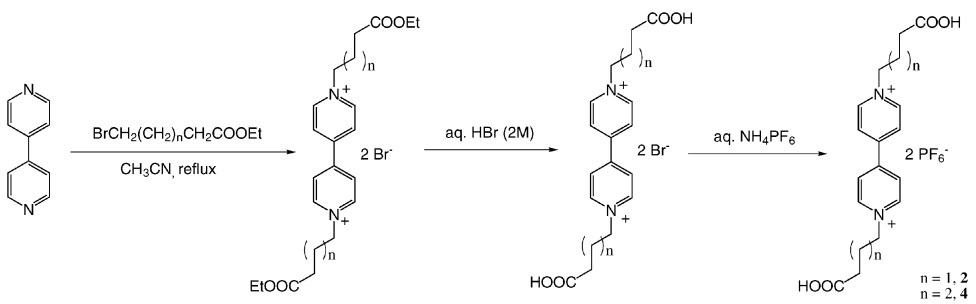

Scheme 1 Preparation of the bipyridinium-based rod molecules.

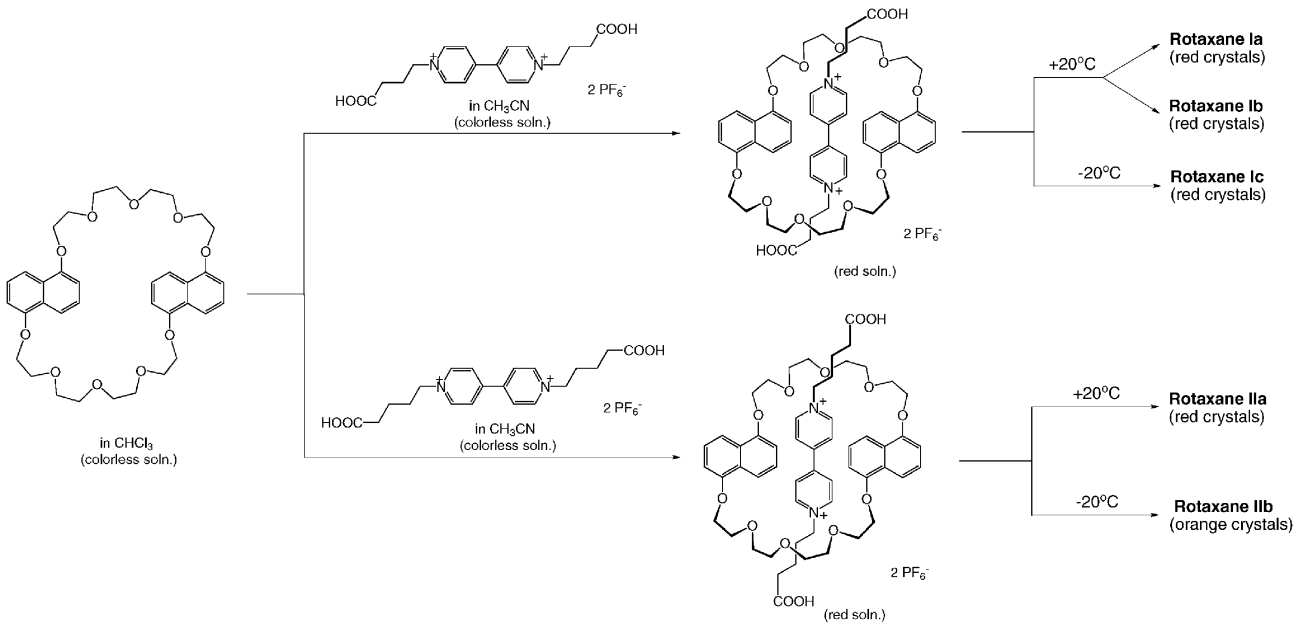

Scheme 2 Preparation of pseudorotaxanes **Ia–c** and **IIa–b**.

to the crown ether ring. In the donor–acceptor core unit, the two naphthalene units are not stacked over the center of the bipyridinium moiety, as in **Ia–Ib**, but are slipped in opposite directions toward the two individual pyridine rings of the latter (Fig. 3). Another difference between the crystal structures of **Ic** and **Ia–Ib** is in the packing of individual pseudorotaxane units in the crystal lattice: while in the case of **Ia** and **Ib** there are no π–π interactions between adjacent pseudorotaxane units, in the case of **Ic** the pseudorotaxanes are stacked into infinite π–π stacked parallel columns. The intermolecular distance of 3.55 Å between naphthalene rings of these stacked **Ic** pseudorotaxanes explains their slightly larger intramolecular π–π separations of 3.40 Å compared to 3.35 Å observed for **Ia** and **Ib** where there is no intermolecular π–π stacking. For all three polymorphs of pseudorotaxane **I**, hydrogen bonding between carboxylic acid groups of adjacent pseudorotaxanes is observed: the carboxylic acid dimer synthon (O···O separations of 2.65 Å) gives rise to infinite hydrogen-bonded pseudorotaxane chains. The structure of these infinite chains is dictated by the orientation of the dicarboxylic acid rods relative to the crown ether (Fig. 5 and 6). In the case of **Ic**, the interplay between hydrogen bonded chains and π–π stacked pseudorotaxane columns gives rise to infinite 2-dimensional sheets.

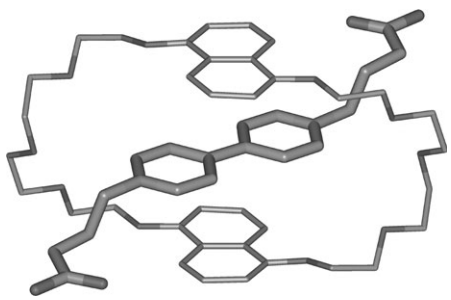

Fig. 1 Structure of pseudorotaxane **Ia** (H atoms and PF_6^- counterions are omitted).

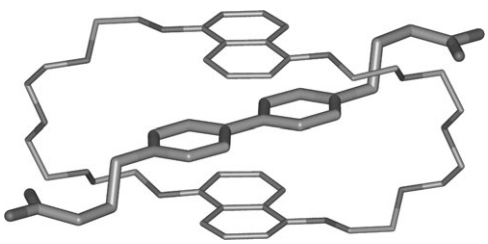

Fig. 2 Structure of pseudorotaxane **Ib** (H atoms and PF_6^- counterions are omitted).

Pseudorotaxanes IIa–b. Pseudorotaxanes with the longer *N*,*N*′-di(5-carboxypentyl)-4,4′-bipyridinium dihexafluorophosphate (**4** · $2PF_6$) rod were prepared similarly to the shorter analog. Likewise, crystals were grown from 2 : 1 CH_3CN–$CHCl_3$ mixtures at room temperature and −20 °C using 2 : 1 bipyridinium rod–crown ether molar ratios. However, the crystal structures obtained at both temperatures turn out to be radically different from the ones obtained with the

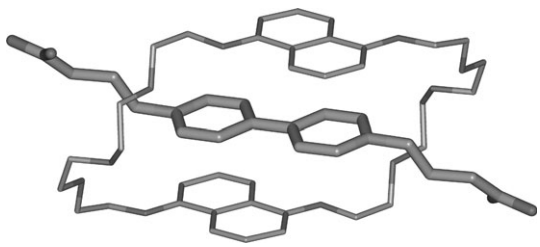

Fig. 3 Structure of pseudorotaxane **Ic** (H atoms, PF_6^- counterions and CH_3CN solvent molecules are omitted).

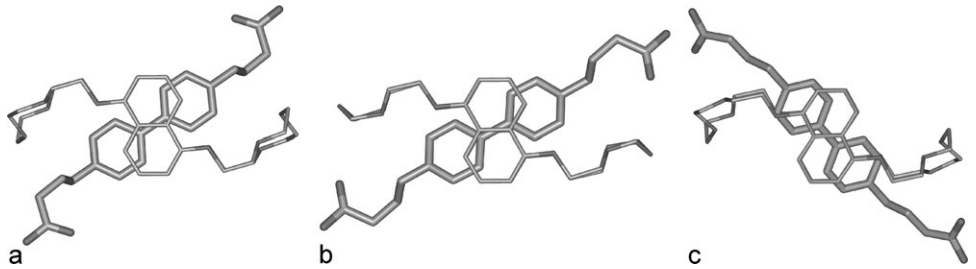

Fig. 4 Comparison of the rod-component orientation relative to the crown ether in pseudorotaxanes **Ia–c**.

shorter rod. In both structures, there is an additional bipyridinium rod incorporated besides the pseudorotaxane. In the structure of $(\mathbf{4})_2$(BN-38-C-10)$(PF_6)_2(H_2PO_4)_2 \cdot CH_3CN \cdot H_2O$ (pseudorotaxane **IIa**), one rod is threaded through the crown ether ring with its bipyridinium moiety sandwiched in-between the two naphthalene rings, forming a π–π stack as in **Ia** and **Ib** and imparting a red color to the compound (Fig. 7). However, the position of the bipyridinium moiety is not symmetrical within the crown ether ring, but is displaced towards one loop; the cavity left in the other loop is occupied by a water molecule, hydrogen-bonded to two O-atoms of the polyetheric chain (O···O separations are 2.86 and 2.90 Å). The second rod is intercalated between two adjacent pseudorotaxane units, forming infinite π–π stacked columns. During the crystal growing process at room temperature, the PF_6^- counterions were apparently hydrolyzed partially, as $H_2PO_4^-$ counterions were also found in the structure of **IIa**, besides the PF_6^- counterions. Although its H-atoms could not be located, the protonation state of the phosphate ion is suggested by both the two shorter (1.45 Å) and two longer (1.53 Å) P–O distances, and charge-balance considerations. These $H_2PO_4^-$ anions form hydrogen bonds to the carboxylic acid groups (O···O distances of 2.65 and 2.73 Å), preventing them from forming dimers as in the case of pseudorotaxanes **Ia–c**.

The most surprising structure is that of $(\mathbf{4})_2$(BN-38-C-10)$(PF_6)_4 \cdot 2CH_3CN$ (pseudorotaxane **IIb**), obtained at −20 °C. The first striking difference was the orange color of the crystals, in contrast to the red color of the other four pseudorotaxanes described above. X-Ray single crystal diffraction revealed an unprecedented structure with two bipyridinium rods threaded through the crown ether ring, but none of them having π–π interactions with the naphthalene units within the same pseudorotaxane (Fig. 8). Here, the two pyridinium rings of both bipyridinium moieties are at a 30° angle to each other, while in the other four pseudorotaxanes they were coplanar. This, in turn, allows the pyridinium rings that are further away from the crown ether to form π–π stacks (3.35 Å) with naphthalene units of adjacent pseudorotaxanes, hence the orange color of the crystals. The other pyridinium ring does not participate in π–π interactions (Fig. 9). The carboxylic acid groups are engaged in hydrogen-bonded dimers (O···O separations of 2.64 and 2.66 Å), forming infinite chains similar to pseudorotaxanes **Ia–c** (Fig. 10).

There are only two other crystal structure reports of pseudorotaxanes based on the bis(1,5-naphtho)-38-crown-10–4,4′-bipyridinium template (although there are a number of catenane structures reported based on the same unit, and related pseudorotaxane structures involving different crown ethers). In the bis(1,5-naphtho)-38-crown-10–4,4′-dimethyl-

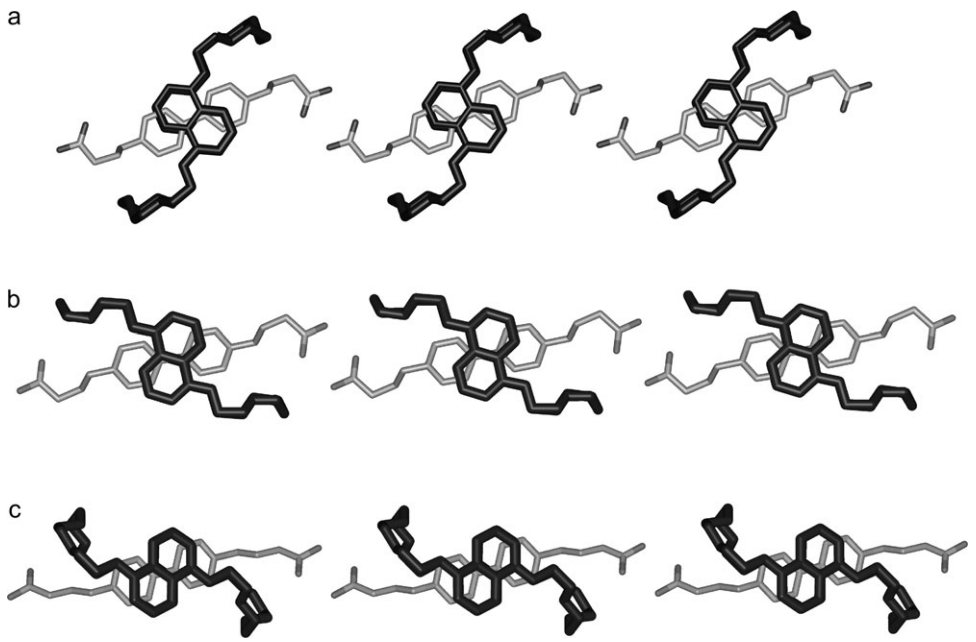

Fig. 5 Hydrogen-bonding patterns in the pseudorotaxane chains of **Ia–c** (top-view). Top **Ia**, middle **Ib**, bottom **Ic**.

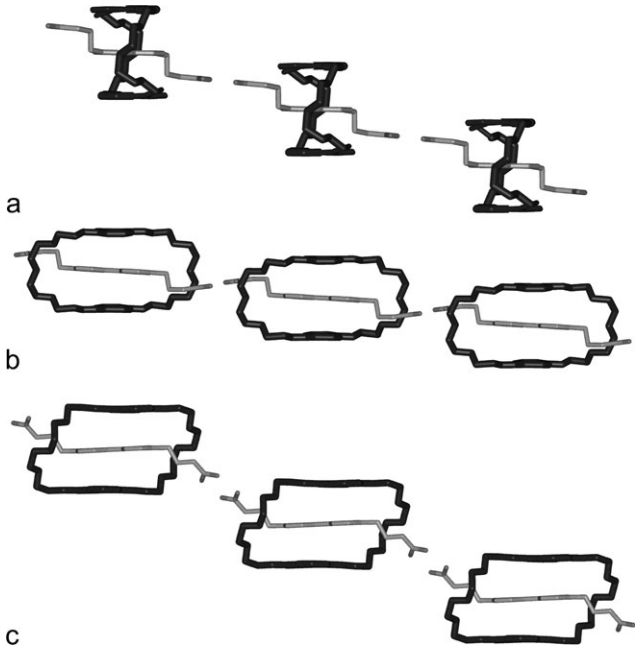

Fig. 6 Hydrogen-bonding patterns in the pseudorotaxane chains of **Ia–c** (side-view). Top **Ia**, middle **Ib**, bottom **Ic**.

bipyridinium pseudorotaxane reported by Stoddart *et al.*,[13] the orientation of the 4,4′-bipyridinium unit relative to the crown ether ring is similar to the one in **Ic** (Fig. 4), although the two naphthalene moieties of the crown ether are positioned symmetrically above and below the center of the bipyridinium moiety, as in the case of **Ia** and **Ib** (Fig. 1 and 2). The π–π stacking separation in this case is 3.50 Å, larger than the 3.35–3.40 Å observed in the case of **I** and **II**. In the second example, a *N*,*N*′-bis[α-[4-(4-pyridyl)pyridinium]-*p*-xylylene]-4,4′-bipyridinium rod is threaded through the bis(naphtho) crown ether.[18] Here the two naphthalene moieties are also stacked over the center of the bipyridinium moiety; however, the phenolic oxygen atoms are not eclipsed, since one naphthalene unit is flipped over relative to the other one. This conformation is also observed in most catenane structures

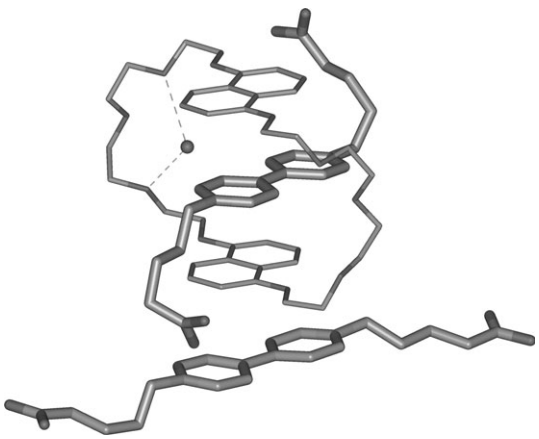

Fig. 7 Side view of pseudorotaxane **IIa** (H atoms, PF_6^- counterions and CH_3CN solvent molecules are omitted). H bonds are indicated by dotted lines.

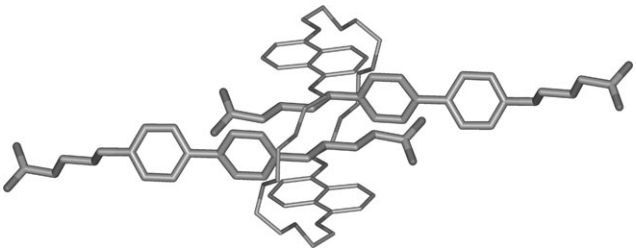

Fig. 8 Top view of pseudorotaxane **IIb** (H atoms, PF_6^- counterions and CH_3CN solvent molecules are omitted).

containing the same bis(1,5-naphtho)-38-crown-10–4,4′-bipyridinium synthon,[19] with some exceptions.[20] It can be concluded that, within this synthon, there is no preferred orientation of the donor and acceptor components relative to each other and the actual conformation can vary depending on the experimental conditions.

UV-Vis, ^{1}H-NMR and ESI-MS studies

Both the rod-component and the ring-component are colorless. When a CH_3CN solution of the rod is mixed with a $CHCl_3$ solution of the ring (2 : 1 ratio), a red color appears immediately (indicating pseudorotaxane formation) and a charge-transfer band centered at 501 nm is observed in the UV-Vis spectrum of **4** · 2PF_6–BN-38-C-10 (2 : 1). Upon cooling, the red color of the pseudorotaxane solution intensifies, the absorbance of the solution increasing from 0.408 at 23 °C to 0.998 at −40 °C. This indicates a shift of the equilibrium towards more pseudorotaxane formation at lower temperatures. However, the position of the band at 501 nm does not shift as the temperature is lowered, indicating that the orange-

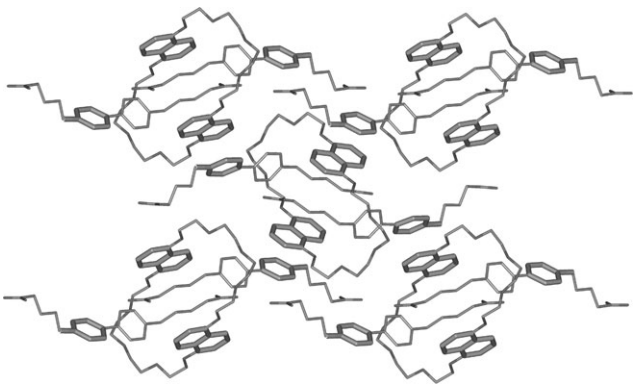

Fig. 9 Packing diagram highlighting the π–π interactions formed in pseudorotaxane **IIb** (H atoms, PF_6^- counterions and CH_3CN solvent molecules are omitted).

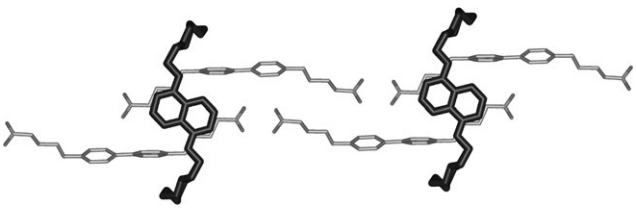

Fig. 10 Illustration of hydrogen-bonding in pseudorotaxane **IIb**.

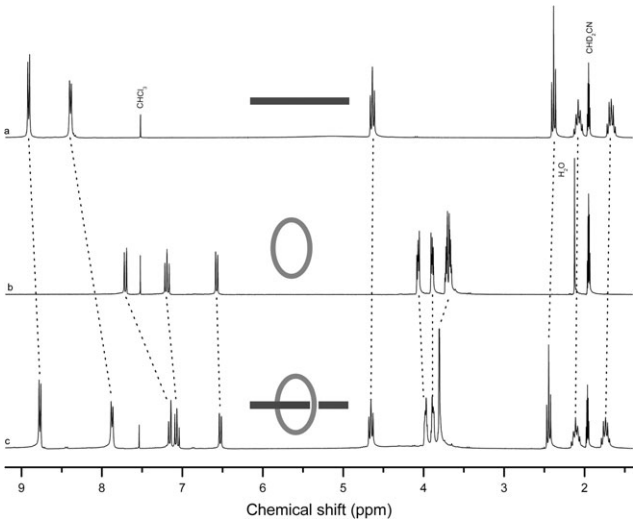

Fig. 11 ^{1}H-NMR spectra of **4** · 2PF$_6$ (a), BN-38-C-10 (b) and a 2 : 1 mixture of the two (c).

colored pseudorotaxane **IIb** is not present in significant amounts in solution. The crystallization of **IIb** at −20 °C from a **4** · 2PF$_6$–BN-38-C-10 (2 : 1) solution, therefore, is a kinetically favored process.

The formation of the pseudorotaxane in solution is also indicated by ^{1}H-NMR spectroscopy. The experiments were carried out in a 2 : 1 mixture of CD_3CN–$CDCl_3$. Upon mixing of **4** · 2PF$_6$ and BN-38-C-10 (2 : 1 molar ratio), significant shifts of the peaks are observed relative to both rod- and ring-components (Fig. 11). Similar results have been reported for a related system.[21] The largest shifts are a 0.52 ppm upfield shift for the bipyridinium protons *meta* to the nitrogen atoms (for the rod-component), a 0.55 ppm upfield shift for the naphthalene protons *para* to the oxygen atoms and a 0.14 ppm downfield shift for the ethylene protons from the center of the tetraethylene glycol loops (for the ring-component). A very similar spectrum is obtained when a 1 : 1 rod–ring mixture is used, with slightly different chemical shifts. These experiments show that at room temperature, the extra rod-component is in fast exchange equilibrium with the pseudorotaxane. Upon lowering the temperature from +23 to −70 °C, a gradual broadening followed by splitting of certain peaks is observed (see ESI, Fig. S1†), indicating a slower exchange at low temperatures. Due to the limited temperature range available (the solvent froze below −70 °C), the exchange rate constant could not be determined.

The ESI-MS spectrum of a 2 : 1 mixture of **4** · 2PF$_6$ and BN-38-C-10 in CH_3CN–$CHCl_3$ (2 : 1) shows peaks that can be attributed to the pseudorotaxane (*m*/*z* 497), ring-component (*m*/*z* 659) and rod-component (*m*/*z* 357), as well as peaks due to fragmentation of the rod at *m*/*z* 179, 341 and 257 (see ESI, Fig. S2†).

Conclusions

Here we have shown that functionalized pseudorotaxanes with carboxylic acid end-groups can be prepared in good yields. Two *N*,*N*′-di(*n*-carboxyalkyl)-4,4′-bipyridinium-type rod components with different lengths have been used. Depending on the temperature of crystallization and the molar ratio between the shorter *N*,*N*′-di(4-carboxybutyl)-4,4′-bipyridinium rod and the crown ether, three different polymorphs of a 1 : 1 pseudorotaxane were obtained (**Ia–c**). The difference between the three structures originates from the different orientation of the rod component relative to the crown ether. In each case, the terminal carboxylic acid groups hydrogen-bond to each other and give rise to infinite chains. With the longer *N*,*N*′-di(5-carboxypentyl)-4,4′-bipyridinium rod, two different 1 : 2 pseudorotaxane-structures were obtained at different temperatures and in the presence of one or two different counterions (**IIa** and **IIb**). When only hexafluorophosphate counterions are present, the carboxylic acid end-groups are hydrogen-bonded to each other, but form hydrogen-bonds to dihydrogenphosphate counterions when the latter are available. Pseudorotaxane **IIb** is a unique example in which the bipyridinium rod is not sandwiched in-between the crown ether's two naphthalene units, as expected, but forms intermolecular π–π interactions with neighboring pseudorotaxanes.

The results of this study provide information about the conditions under which the desired pseudorotaxanes can be prepared. We are currently exploring the binding of these pseudorotaxanes to metallacrown single-molecule magnets, as well as further derivatizing the pseudorotaxane moiety in order to obtain optimal binding characteristics.

Experimental

All commercially available reagents were used as received. Bis(1,5-naphtho)-38-crown-10 (BN-38-C-10) was prepared according to the literature.[22] UV-Vis, ^{1}H-NMR and ESI-MS experiments were carried out on an Ocean Optics SD2000, Varian 500, 400 or 300 MHz and a Waters LCT electrospray-time of flight instrument, respectively.

Bis(1,5-naphtho)-38-crown-10 (BN-38-C-10). ^{1}H-NMR (300 MHz, CD_3CN–$CDCl_3$, 2 : 1, 23 °C) δ 7.70 (d, 4H, ^3J = 8.4 Hz), 7.19 (dd, 4H, ^3J = 7.5 Hz, ^3J = 8.4 Hz), 6.57 (d, 4H, ^3J = 7.5 Hz), 4.07 (m, 8H), 3.90 (m, 8H), 3.72 (m, 8H), 3.67 (m, 8H) ppm.

***N*,*N*′-Di[4-(carboethoxy)butyl]-4,4′-bipyridinium dihydrobromide (1 · 2Br).** 3.00 g 4,4′-bipyridine (19.2 mmol) and 14.99 g ethyl 4-bromobutyrate (76.85 mmol) were refluxed in 60 ml acetonitrile for 28 hours. After cooling to room temperature, the yellow suspension was poured into 100 ml Et_2O, filtered, washed with acetonitrile and Et_2O and air-dried to yield a yellow powder. Two recrystallizations from MeOH–Et_2O provided 8.29 g pure product in 79% yield. ^{1}H-NMR (400 MHz, D_2O, 23 °C) δ 9.17 (d, 4H, ^3J = 7.2 Hz), 8.60 (d, 4H, ^3J = 7.2 Hz), 4.81 (t, 4H, ^3J = 7.2 Hz), 4.15 (q, 4H, ^3J = 7.2 Hz), 2.60 (t, 4H, ^3J = 7.2 Hz), 2.42 (m, 4H, ^3J = 7.2 Hz), 1.25 (t, 6H, ^3J = 7.2 Hz) ppm.

***N*,*N*′-Di(4-carboxybutyl)-4,4′-bipyridinium dihexafluorophosphate (2 · 2PF$_6$).** 8.29 g **1** (15.2 mmol) was dissolved in 20 ml

Table 1 Crystallographic data of **Ia-c** and **IIa-b**[2]‡

	Ia	Ib	Ic	IIa	IIb
Formula	$C_{54}H_{66}F_{12}N_2O_{14}P_2$	$C_{54}H_{66}F_{12}N_2O_{14}P_2$	$C_{62}H_{78}F_{12}N_6O_{14}P_2$	$C_{78}H_{105}F_{12}N_5O_{27}P_4$	$C_{80}H_{102}F_{24}N_6O_{18}P_4$
Formula weight	1257.03	1257.03	1421.24	1896.55	2015.56
Crystal system	Triclinic	Triclinic	Triclinic	Triclinic	Monoclinic
Space group	$P\bar{1}$ (No. 2)	$P\bar{1}$ (No. 2)	$P\bar{1}$ (No. 2)	$P\bar{1}$ (No. 2)	$P2_1/c$ (No. 14)
a/Å	10.797(1)	10.405(2)	11.707(1)	13.642(2)	14.336(2)
b/Å	11.660(1)	11.148(2)	12.121(1)	16.700(2)	16.055(2)
c/Å	13.433(1)	14.021(3)	13.913(1)	20.050(2)	20.135(3)
α/°	69.073(2)	69.539(3)	94.769(6)	85.446(8)	90
β/°	66.558(2)	81.494(3)	110.295(6)	83.877(7)	101.999(9)
γ/°	76.000(2)	74.025(3)	109.052(6)	70.685(7)	90
V/Å^3	1439.2(3)	1462.4(5)	1706.7(3)	4281.4(9)	4533.1(10)
Z	1	1	1	2	2
D_{calc}/g cm^{-3}	1.45	1.427	1.383	1.471	1.477
μ/mm^{-1}	0.18	0.177	0.162	0.196	0.201
$F(000)$	654	654	742	1984	2088
Crystal size/mm	0.42 × 0.40 × 0.32	0.45 × 0.45 × 0.32	0.22 × 0.16 × 0.08	0.16 × 0.10 × 0.10	0.32 × 0.30 × 0.16
Reflections collected	30 512	30 954	32 530	86 695	8424
Unique reflections	7147	7233	6965	11 395	7516
Observed refl. ($I > 2\sigma(I)$)	6056	5701	4452	7850	5633
θ range/°	1.88–28.35	2.01–28.32	1.82–26.41	1.81–22.70	1.93–24.50
Data/restraints/parameters	7147/0/383	7233/0/379	6965/0/439	11 395/0/1152	7516/0/602
R_1; wR_2 ($I > 2\sigma(I)$)	0.0355; 0.0956	0.0592; 0.1653	0.0508; 0.1098	0.0627; 0.1530	0.0436; 0.1091
R_1; wR_2 (all data)	0.0438; 0.1020	0.0748; 0.1782	0.0953; 0.1261	0.1011; 0.1777	0.0667; 0.1192
Goodness-of-fit	1.041	1.02	1.025	0.994	1.092
Largest peak/hole/e Å^{-3}	0.497/−0.371	0.685/−0.620	0.370/−0.328	0.970/−0.522	0.572/−0.402

2M aqueous HBr solution and left standing for 2 days, then evaporated on a water-bath. The solid was taken up into 50 ml Et_2O and then filtered, washed with Et_2O and air-dried. Next, it was dissolved into 20 ml H_2O and a solution of 10 g NH_4PF_6 in 30 ml H_2O was added, causing the precipitation of a white solid. The solid was filtered out, washed with 30 ml aqueous solution containing 10 g NH_4PF_6, then recrystallized from hot water, washed with Et_2O and dried in vacuum. Yield: 8.16 g (87%). ^{1}H-NMR (400 MHz, DMSO-d_6, 23 °C) δ 12.34 (s, 2H), 9.37 (d, 4H, ^3J = 7.2 Hz), 8.77 (d, 4H, ^3J = 7.2 Hz), 4.71 (t, 4H, ^3J = 7.2 Hz), 2.38 (t, 4H, ^3J = 7.2 Hz), 2.23 (m, 4H, ^3J = 7.2 Hz) ppm.

***N*,*N*′-Di[5-(carboethoxy)pentyl]-4,4′-bipyridinium dihydrobromide (3 · 2Br).** Prepared similarly to **1** · 2Br, but using ethyl 5-bromovalerate, in 75% yield. ^{1}H-NMR (400 MHz, D_2O, 23 °C) δ 9.14 (d, 4H, ^3J = 6.8 Hz), 8.57 (d, 4H, ^3J = 6.8 Hz), 4.76 (d, 4H, ^3J = 7.2 Hz), 4.15 (q, 4H, ^3J = 7.2 Hz), 2.48 (t, 4H, ^3J = 7.2 Hz), 2.13 (m, 4H, ^3J = 7.2 Hz), 1.70 (m, 4H, ^3J = 7.2 Hz), 1.24 (t, 6H, ^3J = 7.2 Hz) ppm.

***N*,*N*′-Di(5-carboxypentyl)-4,4′-bipyridinium dihexafluorophosphate (4 · 2PF$_6$).** Prepared similarly to **2** · 2PF$_6$, in 85% yield. ^{1}H-NMR (500 MHz, CD_3CN, 23 °C) δ 8.90 (d, 4H, ^3J = 7.0 Hz), 8.38 (d, 4H, ^3J = 7.0 Hz), 4.63 (t, 4H, ^3J = 7.5 Hz), 2.38 (t, 4H, ^3J = 7.5 Hz), 2.06 (m, 4H, ^3J = 7.5 Hz), 1.65 (m, 4H, ^3J = 7.5 Hz) ppm. ^{1}H-NMR (300 MHz, CD_3CN–$CDCl_3$, 2 : 1, 23 °C) δ 8.91 (d, 4H, ^3J = 7.0 Hz), 8.39 (d, 4H, ^3J = 7.0 Hz), 4.64 (t, 4H, ^3J = 7.5 Hz), 2.39 (t, 4H, ^3J = 7.5 Hz), 2.08 (m, 4H, ^3J = 7.5 Hz), 1.67 (m, 4H, ^3J = 7.5 Hz) ppm.

‡ CCDC reference numbers 633578–633582. For crystallographic data in CIF or other electronic format see DOI: 10.1039/b615273b

Pseudorotaxane I. A solution of 100 mg **2** · PF$_6$ in 6 ml CH_3CN was mixed with a solution of 94 mg BN-38-C-10 in 3 ml $CHCl_3$, resulting in a clear, red solution. Vapor-diffusion of Et_2O at room temperature (20 °C) provided red crystals of (**2**)(BN-38-C-10)(PF$_6$)$_2$ (pseudorotaxane **Ia**) in ~5% yield. Alternatively, a solution of 96 mg **2** · PF$_6$ in 2.5 ml CH_3CN was mixed with a solution of 49 mg BN-38-C-10 in 1 ml $CHCl_3$ and the resulting solution was split into two halves and subjected to Et_2O vapor-diffusion at room temperature and −20 °C, respectively. Red crystals of (**2**)(BN-38-C-10)(PF$_6$)$_2$ (pseudorotaxane **Ib**) were obtained at room temperature in ~70% yield and also red crystals of (**2**)(BN-38-C-10)(PF$_6$)$_2$ · 4CH_3CN (pseudorotaxane **Ic**) at −20 °C in >90% yield.

Pseudorotaxane II. A solution of 100 mg **4** · 2PF$_6$ in 2 ml CH_3CN was mixed with a solution of 49 mg BN-38-C-10 in 1 ml $CHCl_3$, resulting in a clear, red solution. After filtration, the solution was divided into two equal parts and subjected to Et_2O vapor-diffusion, one at room temperature and the other at −20 °C. Red crystals of (**4**)$_2$(BN-38-C-10)(PF$_6$)$_2$(H$_2$PO$_4$)$_2$ · CH_3CN · H_2O (pseudorotaxane **IIa**) were obtained in ~80% yield at room temperature, while orange crystals of (**4**)$_2$(BN-38-C-10)(PF$_6$)$_4$ · 2CH_3CN (pseudorotaxane **IIb**) were obtained in ~90% yield at −20 °C. ^{1}H-NMR of a 2 : 1 mixture of **4** · 2PF$_6$ and BN-38-C-10 (300 MHz, CD_3CN–$CHCl_3$, 2 : 1, 23 °C) δ 8.77 (d, 8H, ^3J = 6.9 Hz), 7.87 (d, 8H, ^3J = 6.6 Hz), 7.16 (d, 4H, ^3J = 8.4 Hz), 7.07 (dd, 4H, ^3J = 7.5 Hz, ^3J = 8.4 Hz), 6.53 (d, 4H, ^3J = 7.2 Hz), 4.66 (t, 8H, ^3J = 8.0 Hz), 3.97 (m, 8H), 3.88 (m, 8H), 3.81 (m, 16H), 2.45 (t, 8H, ^3J = 7.5 Hz), 2.11 (m, 8H), 1.74 (m, 8H) ppm.

X-Ray diffraction and structure determination. Single crystals were mounted on a standard Bruker SMART CCD-based

X-ray diffractometer equipped with a LT-2 low temperature device and normal focus Mo-target X-ray tube (λ = 0.71073 Å) operated at 2000 W power (50 kV, 40 mA). The X-ray intensities were measured at 123(2) K; the detector was placed at a distance of 4.969 cm from the crystals. Frames were collected with a scan width of 0.5° in ω and ϕ. Analysis of the data showed negligible decay during data collection; the data were processed with SADABS and corrected for absorption. The structures were solved employing the Bruker SHELXTL software package[23] and refined by full-matrix least-squares methods based on F^2. All non-hydrogen atoms were refined anisotropically with the hydrogen atoms placed in idealized positions. Crystallographic details are summarized in Table 1.

References

1 (*a*) C. M. Zaleski, E. C. Depperman, J. W. Kampf, M. L. Kirk and V. L. Pecoraro, *Inorg. Chem.*, 2006, **45**, 10022; (*b*) C. M. Zaleski, E. C. Depperman, J. W. Kampf, M. L. Kirk and V. L. Pecoraro, *Angew. Chem., Int. Ed.*, 2004, **43**, 3912.

2 (*a*) J.-P. Collin, V. Heitz and J.-P. Sauvage, *Top. Curr. Chem.*, 2005, **262**, 29; (*b*) V. Balzani, M. Venturi and A. Credi, *Molecular Devices and Machines—A Journey Into the Nanoworld*, Wiley-WCH, Weinhein, Germany, 2003; (*c*) V. Balzani, A. Credi, F. M. Raymo and J. F. Stoddart, *Angew. Chem., Int. Ed.*, 2000, **39**, 3348.

3 (*a*) K. Nørgaard, B. W. Laursen, S. Nygaard, K. Kjaer, H.-R. Tseng, A. H. Flood, J. F. Stoddart and T. Bjornholm, *Angew. Chem., Int. Ed.*, 2005, **44**, 7035; (*b*) H. Murakami, A. Kawabuchi, R. Matsumoto, T. Ido and N. Nakashima, *J. Am. Chem. Soc.*, 2005, **127**, 15891; (*c*) V. Balzani, M. Clemente-León, A. Credi, B. Ferrer, M. Venturi, A. H. Flood and J. F. Stoddart, *Proc. Natl. Acad. Sci. U. S. A.*, 2006, **103**, 1178.

4 (*a*) J.-P. Collin, C. Dietrich-Buchecker, P. Gaviña, M. C. Jimenez-Molero and J.-P. Sauvage, *Acc. Chem. Res.*, 2001, **34**, 477; (*b*) Y. Liu, A. H. Flood, P. A. Bonvallet, S. A. Vignon, B. H. Northrop, H.-R. Tseng, J. O. Jeppesen, T. J. Huang, B. Brough, M. Baller, S. Magonov, S. D. Solares, W. A. Goddard, C.-M. Ho and J. F. Stoddart, *J. Am. Chem. Soc.*, 2005, **127**, 9745.

5 (*a*) J. D. Badjic, V. Balzani, A. Credi, S. Silvi and J. F. Stoddart, *Science*, 2004, **303**, 1845; (*b*) J. D. Badjic, C. M. Ronconi, J. F. Stoddart, V. Balzani, S. Silvi and A. Credi, *J. Am. Chem. Soc.*, 2006, **128**, 1489.

6 R. Hernandez, H.-R. Tseng, J. W. Wong, J. F. Stoddart and J. I. Zink, *J. Am. Chem. Soc.*, 2004, **126**, 3370.

7 M. Feng, X. Guo, X. Lin, X. He, W. Ji, S. Du, D. Zhang, D. Zhu and H. Gao, *J. Am. Chem. Soc.*, 2005, **127**, 15338.

8 Y. Chen, D. A. A. Ohlberg, X. Li, D. R. Stewart, J. O. Jeppesen, K. A. Nielsen, J. F. Stoddart, D. L. Olynick and E. Anderson, *Appl. Phys. Lett.*, 2003, **82**, 1610.

9 H. Yu, Y. Luo, K. Beverly, J. F. Stoddart, H.-R. Tseng and J. R. Heath, *Angew. Chem., Int. Ed.*, 2003, **42**, 5706.

10 (*a*) R. Jäger and F. Vögtle, *Angew. Chem., Int. Ed. Engl.*, 1997, **36**, 930; (*b*) M. C. T. Fyfe and J. F. Stoddart, *Adv. Supramol. Chem.*, 1999, **5**, 1.

11 D. B. Amabilino and J. F. Stoddart, *Chem. Rev.*, 1995, **95**, 2725.

12 J.-P. Sauvage, *Acc. Chem. Res.*, 1998, **31**, 611.

13 P. R. Ashton, F. J. T. Chrystal, J. P. Mathias, K. P. Parry, A. M. Z. Slawin, N. Spencer, J. F. Stoddart and D. J. Williams, *Tetrahedron Lett.*, 1987, **28**, 6367.

14 (*a*) B. Cabezon, J. Cao, F. M. Raymo, J. F. Stoddart, A. J. P. White and D. J. Williams, *Chem.–Eur. J.*, 2000, **6**, 2262; (*b*) H.-R. Tseng, S. A. Vignon, P. C. Celestre, J. F. Stoddart, A. J. P. White and David J. Williams, *Chem.–Eur. J.*, 2003, **9**, 543; (*c*) P. R. Ashton, S. E. Boyd, S. Menzer, D. Pasini, F. M. Raymo, N. Spencer, J. F. Stoddart, A. J. P. White, D. J. Williams and Paul G. Wyatt, *Chem.–Eur. J.*, 1998, **4**, 299.

15 J. A. R. P. Sarma and G. R. Desiraju, in *Crystal Engineering: The Design and Applications of Functional Solids*, ed. K. R. Seddon and M. Zaworotko, Kluwer, Dordrecht, 1999, vol. 539, pp. 325–356.

16 K. R. Seddon, *Cryst. Growth Des.*, 2004, **4**, 1087.

17 (*a*) T. Laird, *Org. Process Res. Dev.*, 2005, **9**, 857; (*b*) K. Kobayashi, A. Sato, S. Sakamoto and K. Yamaguchi, *J. Am. Chem. Soc.*, 2003, **125**, 3035.

18 P. R. Ashton, O. A. Matthews, S. Menzer, F. M. Raymo, N. Spencer, J. F. Stoddart and D. J. Williams, *Liebigs Ann./Recl.*, 1997, 2485.

19 (*a*) D. B. Amabilino, P. R. Ashton, J. A. Bravo, F. M. Raymo, J. F. Stoddart, A. J. P. White and D. J. Williams, *Eur. J. Org. Chem.*, 1999, 1295; (*b*) P. R. Ashton, V. Baldoni, V. Balzani, C. G. Claessens, A. Credi, H. D. A. Hoffmann, F. M. Raymo, J. F. Stoddart, M. Venturi, A. J. P. White and D. J. Williams, *Eur. J. Org. Chem.*, 2000, 1121; (*c*) P. R. Ashton, C. L. Brown, E. J. T. Chrystal, T. T. Goodnow, A. E. Kaifer, K. P. Parry, D. Philp, A. M. Z. Slawin, N. Spencer, J. F. Stoddart and D. J. Williams, *J. Chem. Soc., Chem. Commun.*, 1991, 634; (*d*) K. N. Houk, S. Menzer, S. P. Newton, F. M. Raymo, J. F. Stoddart and D. J. Williams, *J. Am. Chem. Soc.*, 1999, **121**, 1479; (*e*) P. R. Ashton, R. Ballardini, V. Balzani, A. Credi, M. T. Gandolfi, S. Menzer, L. Perez-Garcia, L. Prodi, J. F. Stoddart, M. Venturi, A. J. P. White and D. J. Williams, *J. Am. Chem. Soc.*, 1995, **117**, 11171.

20 (*a*) B. Cabezon, J. Cao, F. M. Raymo, J. F. Stoddart, A. J. P. White and D. J. Williams, *Angew. Chem., Int. Ed.*, 2000, **39**, 148; (*b*) D. B. Amabilino, P. R. Ashton, J. F. Stoddart, A. J. P. White and D. J. Williams, *Chem.–Eur. J.*, 1998, **4**, 460.

21 Y. X. Shen, P. T. Engen, M. A. G. Berg, J. S. Merola and H. W. Gibson, *Macromolecules*, 1992, **25**, 2786.

22 D. G. Hamilton, J. E. Davies, L. Prodi and J. K. M. Sanders, *Chem.–Eur. J.*, 1998, **4**, 608.

23 G. M. Sheldrick, *SHELXTL, v. 6.12*, Bruker Analytical X-ray, Madison, WI, 2001G. M. Sheldrick, *SADABS, v. 2.10, Program for empirical absorption correction of area detector data*, University of Göttingen, Germany, 2003*Saint Plus, v. 7.01*, Bruker Analytical X-ray, Madison, WI, 2003.

